FLOW CHARACTERISTICS OF AN S-SHAPED INLET AT HIGH INCIDENCE

Q.Lin
Xiamen University, Xiamen, China
R.W. Guo
Nanjing Aeronautical Institute, Nanjing, China

Abstract

This paper presents some significant experimental results of the characteristics, including unsteady property, swirl and total pressure distortion of the flow through an S-shaped inlet in a incidence range of 0 ° ~ 85 ° . The experimental results show that if a flow separation occurs at the entry area the fluctuating energy of unsteady flow will transport towards downstream along the duct. In general, the flow quality goes worse during the incidence α increasing. The measurement of the flow field shows that as α increases, the transverse velocity vectors at the exit develop gradually to appear a flow pattern of single vortex instead of the vortex pair at 0 ° incidence. The results also indicate that the strength of the swirl decides the location where the flow quality at exit is the worst. The study explains that, in considering inlet / engine compatibility at high incidence, SC_{60}, DC_{60} and unsteady property are important factors. Besides, it has to be paid more attention that the swirl exerts influence on total pressure distortion and unsteady property of the flow.

I. Introduction

At present, better and better tactical technique of military aircraft is required, so that the incidence may be changed in a large extent, even to 90 ° . Consequently, the flow quality provided by inlet has a great effect on running engine. Besides, the inlet located off the engine axis always is S-shaped for the aircraft so that the complicated duct makes the flow at outlet worse. Therefore, the flow characteristics in complex inlet attract aviation experts' attention. Many investigations have been done[1]~[7]. But the incidence range considered only was limited in 0 ° ~30 ° in published paper related to the flow through S-shaped inlet[3]~[7], and it is not high enough to meet requirement.

With the development of aircraft design,aviation experts have taken some flow quality parameters, such as total pressure distortion, dynamic pressure distribution, for verifying inlet / engine compatibility. Recently,the swirl coefficient SC_{60} is advanced due to the important effect of swirl in S-inlet on the engine, of which the compressor has not guide vanes, has been paid great attention to. In this respect, some investigations gave profitable results about the swirl in S-shaped inlet[3]~[6]. Reference (7) presented some unsteady characteristics of the flow, separating at entrance, through two kinds of S-shaped diffuser, in which the results were obtained at an incidence range of 0 ° ~30 ° .

The characteristics of the flow through a rectangular-round S-inlet at an incidence range of 0 ° ~85 ° have been investigated carefully. Some significant results have been gained involving swirl coefficient SC_{60}, total pressure distortion DC_{60}, total pressure loss η_σ, air flow coefficient Φ, and elementary and correlative properties of dynamic pressure with the variation of incidence. The results demonstrate that there exist the correlations between the flow fluctuations at the entry and the outlet of S-duct when a separation occurs near the bottom wall in the entry range at high incidence. In addition, a peak value of power spectual density (PSD) of dynamic signal of total pressure exists in the flow at outlet section. The flow characteristics at exit of the S-inlet become worse with increase incidence,but not all

parameters vary as incidence monotonically.

Ⅱ. Experiment Explanation

The longitudinal sketch of the test model is shown in Fig.1, the throat of which is a rectangule of 84× 110(mm^2) and the outlet section a circle with diameter of 128mm. The central angles of two opposite centerline arcs of bends are all 35 ° . The radius of centerline arc of the first bend is 230mm, and the one of second bend is 420mm. The area ratio of the diffuser from throat to the end of second bend equals 1.3926. The model is corresponding to a port inlet, of which the wall close to the fuselage side is called inside wall, and the wall opposit the inside wall is called outside wall.

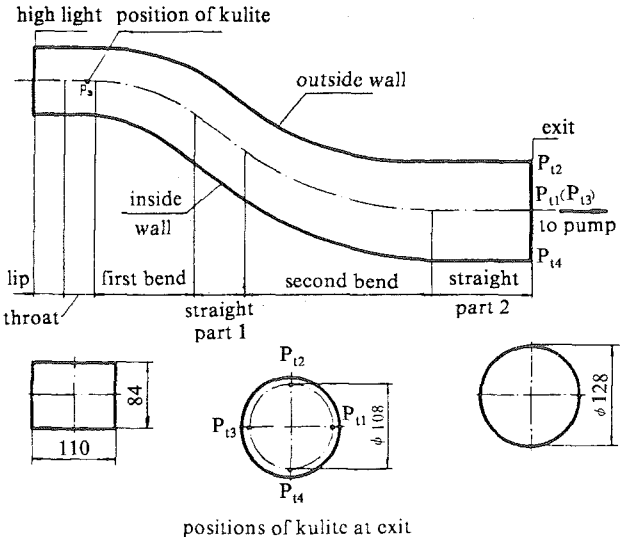

Fig.1 Sketch of the S–duct model

The test model for simulating the flow through an S–inlet at low incidence can be managed in a conventional tunnel. However, there will be difficulty if the incidence is so high that the flow through the duct cannot increase only by translating the control plug of inflow. Therefore, in the investigation the model of S–shaped inlet connected with a pumping set for sucking air through the duct as engine running, was tested in the working section of a blowdown tunnel. The incidence of the model could be changed by mechanism so that the actual behavior of the inlet had been realized. The flow speed of test section of the tunnel is about 62m / s. To maintain the air flow coefficient Φ near 1 at entry of the inlet with pumping set at 0 ° incidence, the flow velocity at the diffuser outlet is much lower than actual flow in aircraft inlet, owing to the low velocity of the free–jet flow. So the experiment cannot simulate actual flow situation in an inlet. Nevertheless, it is still significant as a mechanism investigation.

In the present study the static pressures were measured via the taps along the symmetrical line of the model walls. The flow field at outlet of the duct was measured by a movable trihole–probe rake. From measurement the distributions of three velocity components, total pressure and static pressure were got as a result that flow parameters, such as SC_{60}, DC_{60}, η_σ and Φ, were also obtained. Two kulite dynamic pressure transducers were set at the centre line of the bottom wall at throat and the exit section of the inlet respectively (See Fig.1) for measuring the dynamic signals of static pressure P_s at entry and total pressure P_t at the outlet section. During testing, total pressure dynamic transducer was turned successively to point P_{t1}, P_{t2}, P_{t3}, and P_{t4}, which are equidistantly close to the upper, outside, bottom and inside walls of the duct at the exit. The dynamic signals recorded were analysed by CF–920 dynamic analyzer to gain relative unsteady flow characteristics that are elementary property of two dynamic signals, i.e. PSD, and their correlative property, i.e. cross–correlativity. The maximum root mean square (RMS) of total pressure dynamic signal was gained by RMS meter.

Ⅲ. Experimental Result

The flow field in the outlet section of the S–shaped inlet has been measured at an incidence range of 0 ° ~ 85 ° . The flow characteristics obtained are given as follows.

1. Swirl

It is known that there is secondary flow in the S–duct because of the existence of pressure gradient and viscosity in the flow. The transverse flow, i.e. swirl, measured in the outlet section of the duct develops as the incidence increases.

The transverse velocity vectors of the flow in outlet section of the S–inlet show a typical vortex pair at 0 ° incidence[8].However, when the incidence increases to

30 ° the transverse flow pattern at outlet appears to be a counterclockwise vortex instead of the vortex pair (See Fig.2). The transverse velocity vectors get longer that means swirl develops intensively with incidence increasing. Fig.3 shows how swirl coefficient SC_{60} increases versus incidence α.

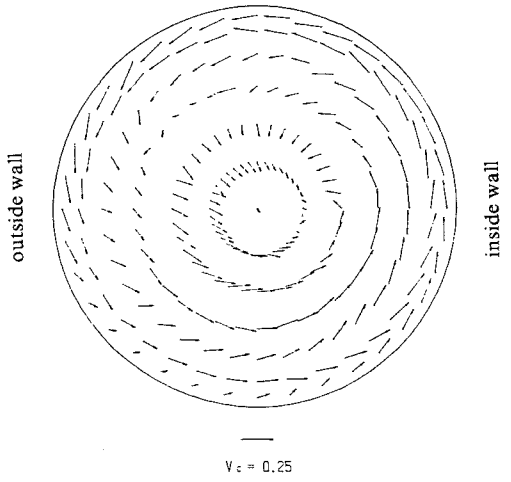

Fig.2 Transverse velocity vectors in outlet section

It is found by visualization that a recirculation in the flow arises at throat area on bottom wall to form a counterclockwise bulk vortex when the incidence is high enough. The axis, vertical to bottom wall, of the bulk vortex turn to parallel with bottom wall, compeled by predominant flow. The vortex just like a tornado goes into the duct and drives the duct flow rotating together towards downstream. It implies that the swirl in an S–duct is made up of the bulk vortex and a vortex pair.

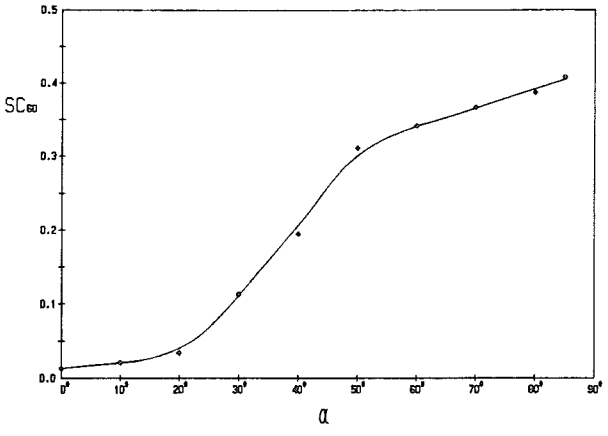

Fig.3 Swirl coefficient SC_{60} versus incidence α

In Fig.3, SC_{60} grows quickly when the incidence increases from 20 ° to 50 °,that explains the separation of the flow and then the bulk vortex develop rapidly. As the incidence is higher than 50 ° , the swirl coefficient SC_{60} climbs slowly in the curve because the separation is bound by duct walls.

2. Tolal Pressure Distortion

Fig.4 shows the distribution of total pressure coefficient $C_p(=\frac{P-P_\infty}{\frac{1}{2}\rho V^2})$ in the outlet section of the duct at 0 ° incidence. There is some little pressure loss near inside and outside walls. The distribution of C_p at 0 ° incidence corresponds to vortex pair of transverse flow symmetrically up and down. The separation occurs at the entrance and pressure loss increases as incidence becomes higher. Fig.5 gives the distribution of total pressure coefficient in outlet at 30 ° incidence. The higher incidence, the more serious the overall loss of total pressure at outlet. Fig.6 shows the variation of average total pressure coefficient η_σ with incidence α. Corresponding to Fig.3, η_σ decreases so far as to go down linearly. But in Fig.7, the curve of total pressure distortion coefficient DC_{60} against α is not monotonically, in which there is a valley nearby 70 ° incidence. It means that the distribution of total pressure turns to smooth at 70 ° incidence even though the pressure loss is still high. From the distribution of total pressure coefficient C_p at every incidence, it can be found that the swirl not only changes the high and low–pressure areas, but also their relative positions with the variation of incidence α[8].

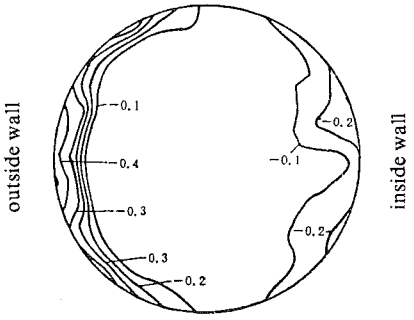

Fig.4 Total pressure coefficient in outlet section as $\alpha = 0$ °

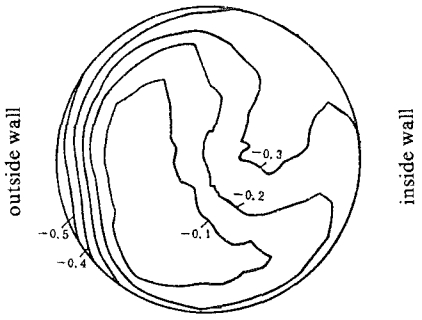

Fig.5 Total pressure coefficient in outlet section as $\alpha = 30°$

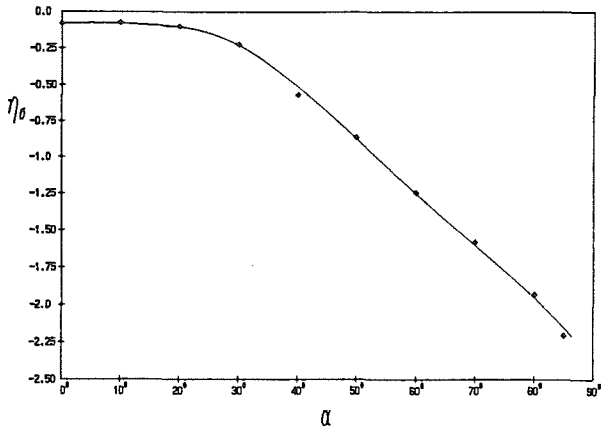

Fig.6 Average total pressure loss η_σ varying with α

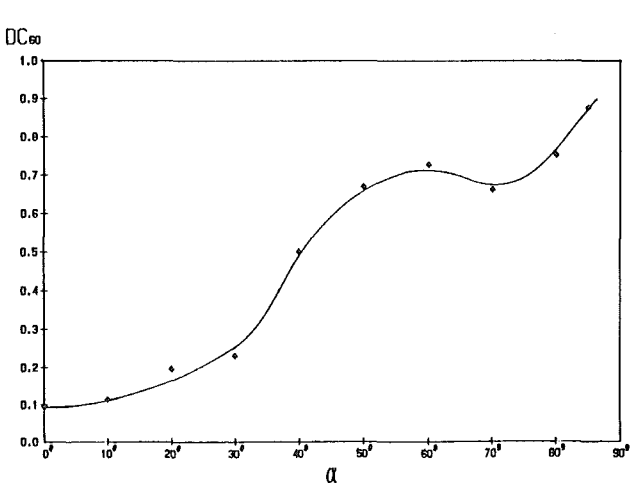

Fig.7 Total pressure distortion DC_{60} versus α

3. Air Flow

Fig.8 shows that if the free jet velocity and suction of the pumping set are constant the relative air flow Φ will reduce with the increase of α. It indicates that when the incidence increases severely with constant engine rate in actual flight, the thrust would fall greatly. Therefore, the controlling techniques to flow field are necessary.

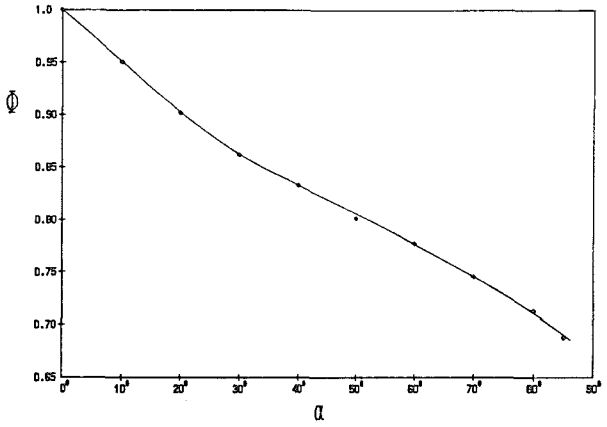

Fig.8 Air flow coefficient Φ versus α

4. RMS_{max} of Total Pressure P_t

It is found that the distribution of RMS value of total pressure fluctuation is not uniform in the outlet section of the S–duct. The dynamic signals of total pressure P_t at P_{t1},P_{t2},P_{t3},P_{t4} points were measured at various incidence.Then the maximum RMS values of total pressure dynamic signal for four positions at each incidence are taken to calculate $\overline{RMS}_{max}$ ($=(RMS_{max})_\alpha / (RMS_{max})_{\alpha=0°}$).

It can be found that the location of RMS_{max} point moves counterclockwise with the incidence increasing, just like the rotating direction of the swirl in the outlet.

Fig.9 shows how the RMS_{max} of P_t changes as incidence α increases. It is seen that the RMS_{max} grows up first and down later with the incidence. The RMS_{max} value at 20° incidence is 20 per cent more than that at 0° incidence. But at 60° incidence it is 4.2 times as much as that at 0° incidence so that the total pressure fluctuation in the outlet of the S–duct caused by the flow separation at the entry area should be paid more attetion to. However, the value of RMS_{max} descendes after the incidence is higher than 60° . Perhaps, the very strong swirl makes the distribution of total pressure in the outlet uniform.

5. Elementary Property

The elementary property, i.e. power spectral density (PSD), of the dynamic signals P_s and P_t has been measured at the entrance and outlet of the duct.

At low incidence the PSD curves of P_s and P_t are smooth, and they are all broad–band signals on the

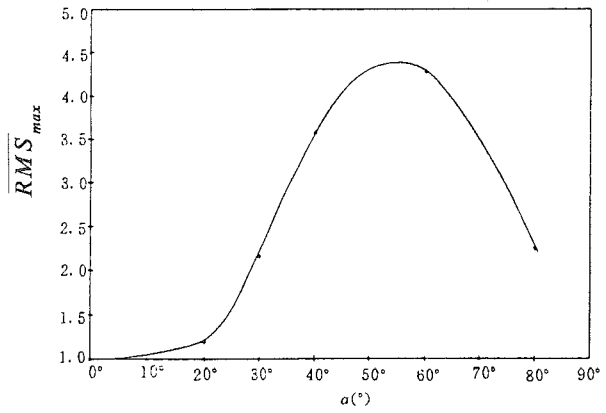

Fig.9 $\overline{RMS}_{max}$ versus α

whole. When α = 20 ° , P_t is still broad–band signal but the PSD curve of P_s has a peak at 145 H_z (See Fig.10 in which signals A and B stand for P_s and P_t respectively.), which illustrates that the local separation of the flow has little effect on the flow downstream. At 40 ° incidence, there is quite high fluctuation energy around 125 Hz in the PSD curve of P_t . However, two dynamic signals are all narrow–band at 60 ° incidence. As Fig.11 the PSD curves of the signals show the high fluctuating energy concentrating at 125Hz. Especially, there is a very high peak value in the PSD curve of P_t as more than four times high as that of P_s . When incidence increases to 80 ° the total pressure exists higher fluctuating energy about 97.5Hz, but the dynamic signal of P_s becomes broad–band again. From the figures of PSD at various incidence, it can be observed that there is always higher fluctuating energy at a frequency in total pressure signal except incidence lower than 20 ° , and the fluctuating energy goes up with the incidence increasing and down when the incidence is higher than 60 ° .

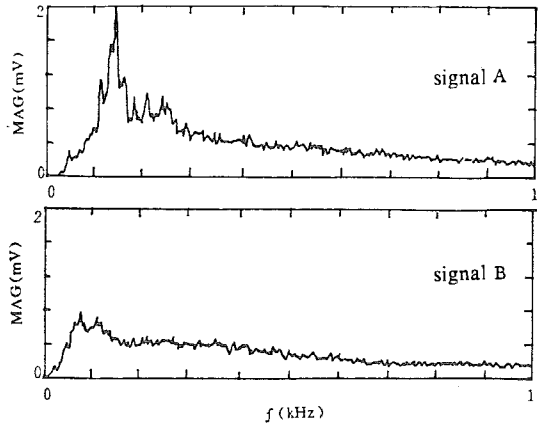

Fig.10 PSD of P_s and P_t as α = 20 °

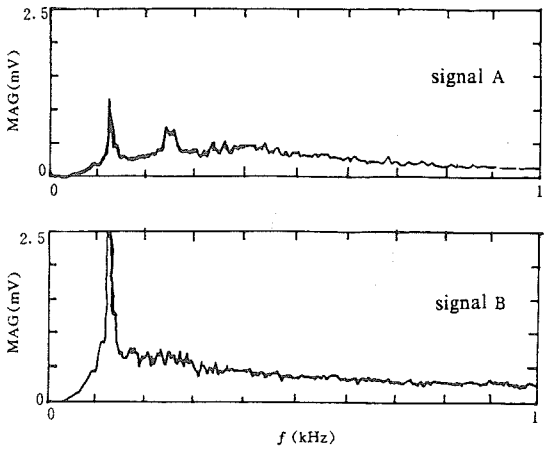

Fig.11 PSD of P_s and P_t as α = 60 °

6. Correlative Property

The correlativity between two dynamic signals, P_s and P_t , is discussed as following, which indicates how close the interrelation of the signals is.

At 0 ° incidence it seems that there is no interrelation between P_t and the flow fluctuation at the entrance. The maximum cross–correlative coefficient happens delaying 17.97ms to static pressure signal at 20 ° incidence.

For the situation of 40 ° incidence as Fig.12, the maximum cross–correlative coefficient of P_s and P_t is 0.0482. It is almost equal to that at 20 ° incidence, but delay time is 12.89 ms which shortens about one third time than 17.97ms. It is seen from Fig.12 that there is a peak of larger cross–correlative coefficient about every 80 ms. It expresses that the period of pressure pulse transfered from the entrance to the exit is about 80 ms. This phenomenon is not found at 20 ° incidence, at which the pressure pulse is transfered in the flow from the entry to outlet of the duct at longer intervals.

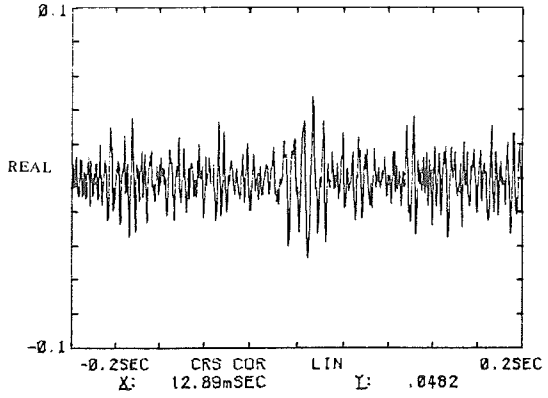

Fig.12 Cross–correlation between P_s and P_t as α = 40 °

It can be judged from Fig.11 that the total pressure P_t at outlet is most closely related to static pressure P_s at entrance as $\alpha = 60°$. In Fig.13 the cross-correlative coefficient of two signals attains to 0.35 which is much larger than those at 20° and 40° incidences. The cross-correlatograph in Fig.13 seems a sine curve that demonstrates the pressure pulse at entrance transfers towards downstream along the duct in a constant frequency to affect the total pressure at the outlet. The response period of total pressure in the outlet corresponding to the pressure pulse at entry area is about 7.8ms.

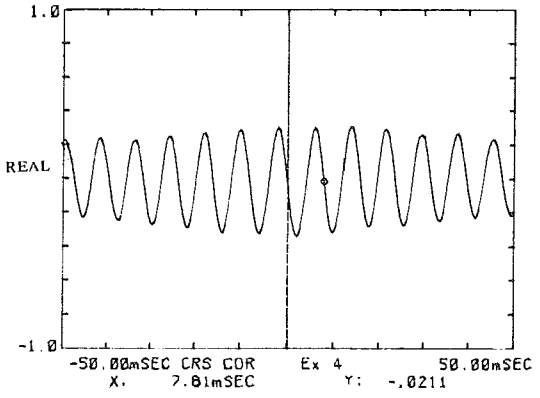

Fig.13 Cross-correlation between P_s and P_t as $\alpha = 60°$

When incidence increases to 80°, the two dynamic signals still have cross-correlation even though the energy of the fluctuation becomes weak.

Just as the location of RMS_{max} point changes, so the position of the closest correlation between P_s and P_t turns counterclockwise with incidence. Therefore, it seems that the swirl also determines the position where the total pressure fluctuation is the strongest in the flow of outlet section.

IV. Conclusion

According to the experimental reslults obtained for S-inlet model with pumping set tested in blowdown tunnel at 0° ~ 85° incidence range, the flow characteristics can be concluded as follows:

1. As α increases, the transverse velocity vectors at the exit develop gradually to appear a flow pattern of a single vortex instead of the vortex pair at 0° incidence. With the incidence increasing from 0° ~ 85°, the swirl coefficient SC_{60} always increases.

2. Average total pressure coefficient η_σ decreases continuously with the incidence increasing, so does the air flow coefficient Φ, But the total pressure distortion coefficient DC_{60} goes up from 0° to 60° incidence and comes down around 70°, then rises again at very high incidence.

3. The fluctuating energy of the total pressure at the outlet grows up unceasingly as increase α. At 60° incidence, the PSD of P_t shows a narrow-band signal and has very high peak. When $\alpha > 20°$, there is local peak between 50~ 150 Hz in the PSD curve of P_t. The PSD value of P_t descends at 80° incidence.

4. After $\alpha \geqslant 20°$, two dynamic signals are correlative, and the cross-correlation strengthens as the incidence increases. The closest cross-correlation occurs at 60° incidence. But as $\alpha = 80°$, the corss-correlativity becomes weak.

5. RMS_{max} of total pressure of the flow in the outlet section goes up with increasing α and down when $\alpha \geqslant 55°$.

6. When α is higher than 20°, the separation region at the entrance area of the S-diffuser throws vortex lump with large fluctuating energy to downstream at a frequency. Especially, at 60° incidence the flucluation is near a sine signal, and the pulse energy of thrown vortex lump also remains unvaried.

7. The positions of RMS_{max} of P_t and the strongest cross-correlation of P_s and P_t move in the way of swirling flow. It means that the strength of the swirl decides the position where the flow quality in outlet section is the worst.

References

1. F. Aulehla, Intake Swirl——A Major Disturbance Parameter in Engine / Intake Compatibility. ICAS-82-4.8.1

2. C.P. Stocks & N.C. Bissinger, The Design and Development of the Tornado Engine Air Intake. AGARD paper

3. R.W. Guo & J. Seddon, The swirl in an S-Duct of Typical Air Intake Properties. The Aeronautical Quarterly, May 1983.

4. R.W. Guo & J. Seddon, Swirl Characteristics

of an S–shaped Air Intake with both Horizontal and Vertical Offsets. The Aeronautical Quarterly, May 1983.

5. J. Seddon, Understanding and Countering the Swirl in S–Ducts: Tests on the Sensitivity of Swirl to Fences. The Aeronautical Quarterly, April 1984.

6. A.D. Vakili, J.M. Wu, P. Liver & M.K. Bhat, Flow Control in a Diffusing S–Duct. AIAA–85–0524.

7. R.W. Guo & J. Seddon, Some Unsteady Flow Characteristics of Two S–shaped Intake Models Tested at High Incidence. Journal of NAI, English Edition Vol.1 No.1 1982.

8. Q.Lin, Numerical Analysis and Experimental Investigation for the Characteristics of Flow through a Rectangular–Round S–Shaped Diffuser. Doctoral thesis in Nanjing Aeronautical Institute, 1988.